1350–1358 *Nucleic Acids Research, 1999, Vol. 27, No. 5*

Binding of the glucose-dependent Mig1p repressor to the *GAL1* and *GAL4* promoters *in vivo*: regulation by glucose and chromatin structure

Elena Frolova, Mark Johnston[1] and John Majors*

Department of Biochemistry and Molecular Biophysics and [1]Department of Genetics, Washington University School of Medicine, 660 South Euclid, St Louis, MO 63110, USA

Received November 12, 1998; Revised and Accepted January 5, 1999

ABSTRACT

Binding of the MIG1 repressor to the glucose-repressible *GAL1* and *GAL4* promoters was analyzed *in vivo* by cyclobutane dimer footprinting in two yeast strains that show different glucose repression responses. Mig1p binding to the two promoters in both strains was glucose-induced. In cells subject to rapid and stringent glucose repression (S288c), long-term Mig1p binding in glucose-grown cells was inhibited by the formation of a competing chromatin structure. Under conditions where glucose repression was only partially effective (*gal80*$^{-}$ or low glucose), the chromatin structure did not form and long-term Mig1p binding was observed The same long-term binding of Mig1p was seen in cells of a different strain (W303A) that shows only partial glucose repression of the *GAL1* promoter. We conclude from these experiments that Mig1p binding to glucose-repressed promoters is glucose-dependent but transient. We suggest that Mig1p functions at an early step in repression, but is not required to maintain the repressed state.

INTRODUCTION

Cells of the yeast *Saccharomyces cerevisiae* prefer to ferment glucose and rapidly alter patterns of gene expression in response to carbon source availability (1). Expression of many genes is repressed by glucose, including those involved in the metabolism of other fermentable sugars like sucrose or galactose, or of non-fermentable carbon sources like ethanol or glycerol, as well as genes required for gluconeogenesis and mitochondrial oxidative phosphorylation. Major questions that must be answered before the mechanism(s) of glucose repression will be understood are: (i) how does the cell sense glucose; (ii) what is the signaling system by which the sensor delivers a repression signal to the promoters of affected genes; (iii) how does delivery of this signal result in decreased promoter activity? Genes whose functions are required for glucose sensing, signal transduction and promoter repression have been identified. A major effector of repression is Mig1p (2,3), a C_2H_2 zinc-finger protein that binds to sites in several glucose-repressible promoters (4). Mig1p is thought to act by recruiting the Tup1p/Ssn6p general repressor complex to target promoters (5–7). How glucose is sensed and affects the function of the Mig1p/Ssn6p/Tup1p complex is not completely understood, but some clues are available. A protein kinase composed of Snf1p and Snf4p is required for derepression of Mig1p repressed promoters (8) and a protein serine/threonine phosphatase, Glc7p, and a protein that associates with it, Reg1p, are required for glucose-induced repression (9). The phosphorylation state of Mig1p is glucose-dependent (5,10) and it is probably a direct target of Snf1p/Snf4p (11). Significantly, subcellular localization analysis shows that transport of Mig1p into and out of the nucleus is regulated by glucose and the phosphorylation state of the protein correlates closely with its cellular compartmentalization (10).

Among the best-studied glucose-repressible genes are those responsible for galactose metabolism (1,12). Transcription of *GAL4*, which codes for the galactose-regulated transcriptional activator Gal4p, is repressed 4- to 5-fold by glucose (13–15), mediated by an upstream repression site (URS) (13) to which Mig1p binds *in vitro* (3). In contrast, expression of *GAL1* galactokinase, which catalyzes the first step in galactose metabolism, is repressed as much as 1000-fold by glucose. Three factors account for this high degree of repression: decreased Gal4p synthesis and cooperative Gal4p binding to multiple binding sites in the *GAL1* promoter account for 40-fold repression; Mig1p binding to two sites in the *GAL1* promoter causes 4-fold repression and Gal80p, which binds to Gal4p and inhibits its ability to activate transcription under non-inducing conditions, accounts for the remaining 5- to 10-fold repression (15,16). We and others have used various probes and footprinting procedures to analyze protein–DNA interactions at the *GAL1* promoter *in vivo* (17–24). These studies have shown that: (i) Gal4p can bind to the *GAL1* promoter under both induced and uninduced conditions (19,21); although glucose rapidly represses promoter function, Gal4p binding to the *GAL1* promoter is only lost when cells are grown in glucose for extended times; (ii) repression of the *GAL1* promoter is accompanied by the formation of a positioned nucleosome that lies between the Gal4p binding sites and the *GAL1* TATA element and includes the Mig1p binding sites (22,25). None of these analyses has revealed a Mig1p footprint under either inducing or repressing conditions. Our objective in this study was first to find a procedure for detecting Mig1p binding to the *GAL1* and *GAL4* promoters and then to use that procedure to investigate *in vivo* the role of Mig1p binding in glucose repression of these promoters.

*To whom correspondence should be addressed. Tel: +1 314 362 1135; Fax: +1 314 362 7183; Email: majors@biochem.wustl.edu

MATERIALS AND METHODS

Strains

YM262 (MATα, *ura3-52, ade2-101, his3-Δ200, tyr1-501, lys2-801*)
YM654 (MATα, *ura3-52, ade2-101, his3-Δ200, tyr1-501, lys2-801, gal80-Δ538*)
W303α (MATα, *ade2-1, ura3-1, his3-11,15, trp1-1, leu2-3,112, can1-100*)
BJ2168 (MAT**a**, *ura3-52, trp1-289, leu2-3,112, prb1-1122, rpc1-407, pep4-3*)

Purification of Mig1p

Bacterially expressed recombinant Mig1p was a gift from M. Devit. Mig1p-enriched yeast cell extracts were made from a protease-deficient yeast strain, BJ2168, transformed with a multicopy *MIG1* plasmid (2). Cells were grown to log phase in YPD medium, harvested and disrupted with glass beads in a blender. The resulting extract was cleared by centrifugation, DNA was removed by precipitation with 10% PolyminP and then protein was precipitated with ammonium sulfate (to 60%). The pellet from the ammonium sulfate precipitation was resuspended, desalted on a Sephadex G-25 column and fractionated on a heparin–agarose column. Mig1p, detected by gel-shift assay with a *GAL1* promoter fragment, was found in fractions eluting at 0.6 and 0.7 M ammonium sulfate. Those fractions were dialyzed into 50 mM Tris–HCl, pH 7.6, 10 mM $MgCl_2$, 10 mM KAc, 20 µM $Zn(Ac)_2$, 10% glycerol, 1 mM DTT, 1 mM PMSF and stored at –70°C.

DNase I protection assays and UV footprinting *in vitro*

5′-End-labeled DNA fragments containing Mig1p binding sites were prepared by PCR of genomic DNA (YM262) using 5′-^{32}P-labeled primers (see below): G1-3 and G1-6 for the *GAL1* promoter (fragment extends from –312 to –27) or G4-3 and G4-4 for the *GAL4* promoter (fragment extends from –138 to +23). Binding reactions were carried out in 50 µl final volume containing 50 mM Tris–HCl, pH 7.6, 5 mM KAc, 5 mM $MgCl_2$, 10% glycerol, 1 mM DTT, 1–2 µg poly(dU-dI), 2–5 µg poly(U-I), ~0.05 pmol of [^{32}P]DNA fragment and an appropriate amount of protein extract. The binding mixture without DNA fragment was pre-incubated for 15 min at 4°C. The whole binding reaction was incubated for 30 min at 4°C.

For DNase footprinting, 1 µl DNase I (3 U/µl; Boehringer Mannheim) was added to the binding reaction; digestion was carried out for 1 min and stopped by addition of 50 µl of stop mix (40 mM EDTA, 0.4 M NaCl, 1% SDS, 3 µg of yeast tRNA) followed by extraction with phenol/chloroform (50/50, pH 8.0).

For UV footprinting the binding mixture was irradiated for 2 min on ice as described (17,26). After extraction with phenol/chloroform (50/50, pH 8.0), samples were precipitated with ethanol, resuspended in 20 µl of endoV cleavage mixture (27), incubated for 1 h at 37°C, extracted with phenol/chloroform (50/50, pH 8.0) and precipitated with ethanol.

For electrophoresis each sample was dissolved in 3 µl loading solution (50% TE, 50% formamide, 0.1 mg/ml xylene cyanol, 0.1 mg/ml bromophenol blue). The samples were analyzed on a 6% sequencing gel (8 M urea, 19:1 acrylamide:bisacrylamide). After electrophoresis, fragments were transferred to 3MM filter paper which was dried and autoradiographed with Kodak Bio-Max film or with a phosphorimager screen.

UV footprinting *in vivo*

Cells were grown at 30°C to an A_{600} = ~2–3 OD in an appropriate medium. The culture (volume 25–30 ml) was harvested by centrifugation, resuspended in 3 ml SM with an appropriate sugar and irradiated as described (17,26). After irradiation the cells were pelleted by centrifugation, resuspended in 1 ml of 1 M sorbitol, 1 mM EDTA and converted to spheroplasts at 30°C using lyticase. DNA was purified by adsorption to a Qiagen G/20 column and cleaved at cyclobutane dimer modified sites with T4 endoV and photolyase as described (27). Ligation-mediated PCR was carried out as described (28) and gel analysis was carried out as described above. Oligonucleotide primers used for LMPCR were the following:

For the *GAL1* promoter:
Bottom strand
primer 1 (G1-1), GAGCCCCATTATCTTAGCC, (–474 to –456);
primer 2 (G1-2), CTTAACTGCTCATTGCTATATTG, (–419 to –397);
primer 3 (G1-3), TTCCTGAAACGCAGATGTGCC, (–312 to –292);
Top strand
primer 1 (G1-4), GAGATTTAGTCATTATAG, (+75 to +73);
primer 2 (G1-5), CTCCTTGACGTTAAAGTATAGAGG, (+36 to +59);
primer 3 (G1-6), CAAACCGAAAATGTTGAA, (–44 to –27).

For the *GAL4* promoter:
Bottom strand
primer 1 (G4-1), ACCTTCTATAATTTCAAAGTATTT, (–210 to –187);
primer 2 (G4-2), GTATCAGTTTAATCACCATAATA, (–170 to –154);
primer 3 (G4-3), AGTGCAATTAATTTTTCCTATTG, (–138 to –116);
Top strand
primer 1 (G4-4), GACACTTGGCGCACTTCGG, (+3 to +23);
primer 2 (G4-5), TTGTTCGATAGAAGACAG, (+33 to +50);
primer 3 (G4-6), CTTTCAGGAGGCTTGCTTCTC, (+98 to +117).

For each set, primer 1 was used for the first extension step, primer 2 was used for the PCR amplification step and primer 3, labeled at the 5′-end with [γ-^{32}P]ATP and T4 polynucleotide kinase, was used for the final primer extension step. The ligation oligonucleotide was identical to that described (28).

RESULTS

We used ligation-mediated PCR (LMPCR) and UV photofootprinting (17,19,27,29–31) to probe for Mig1p binding to the *GAL1* promoter under different growth conditions and in different genetic backgrounds. UV irradiation of DNA induces formation of photoproducts, principally cyclobutane dimers and 6–4 products, which are formed at sites of adjacent pyrimidine bases. Photofootprinting takes advantage of the observation that proteins binding to DNA alter the extent to which these products form. These effects probably result from protein-dependent changes in the structure or the conformational flexibility of the DNA (19,27,30,31). Because DNA strands can be selectively cleaved at modified sites (hot piperidine cleaves at 6–4 sites and phage T4 endoV cleaves at cyclobutane dimers), patterns of photoproduct formation along sequences and footprints that result from protein association to specific sites along those sequences are easily determined.

UV footprinting of Mig1p binding to the *GAL1* promoter *in vitro*

For analysis of Mig1p binding we chose to detect only cyclobutane dimers and we refer to the pattern of UV-induced cyclobutane dimers as the 'UV pattern', the 'UV footprint' or the 'photofootprint'. To identify a photofootprint of Mig1p at the *GAL1* promoter, we first analyzed Mig1p binding *in vitro* using either a truncated form of Mig1p made in *Escherichia coli* or a partially purified extract made from yeast cells that overproduced Mig1p (described in Materials and Methods). Mig1p in both preparations showed specific binding to a *GAL1* promoter fragment in gel-shift experiments (data not shown).

Figure 1 shows the sequence of the *GAL1* and *GAL4* promoters with important landmarks. Figure 2A shows DNase I and UV patterns for both strands of a *GAL1* promoter fragment (from –312 to –27) in the presence or absence of recombinant Mig1p. To document Mig1p binding by a traditional criterion, a DNase I protection assay was also performed. This assay revealed (Fig. 2A, lanes 9–11) two Mig1p sites (the URSA and URSC elements of ref. 32). Mig1p binding to the two sites was not equivalent: site A was protected from digestion by as little as 2 µg of recombinant Mig1p; site C required 10 µg of recombinant Mig1p for partial protection and generation of a hypersensitive band. We conclude that Mig1p binds to site C with lower affinity than to site A. In previous experiments no binding to site C was detected (3). Figure 2A also shows the effect of Mig1p on the UV pattern. A protein-free UV pattern of site A shows three bands on the top strand corresponding to T^{-134}, T^{-133} and C^{-132} (Fig. 2A, lane 2), where the T^{-133} band is the strongest, and three bands of about equal intensity on the bottom strand corresponding to C^{-128}, C^{-129} and C^{-130} (Fig. 2A, lane 6). (Note: in our description of these results, the base associated with each band is the 3′ base of a pyrimidine dimer sequence.) Mig1p binding to site A significantly increased the intensity of C^{-128} (circle in Fig. 2C) and decreased the intensities of C^{-129} and C^{-130} (squares in Fig. 2C) on the bottom strand (Fig. 2A, lanes 7 and 8). On the top strand the intensity of T^{-133} decreased and a new band at T^{-131} became apparent (Fig. 2A, lanes 3 and 4, and C). There was no effect of Mig1p binding on the UV pattern of the bottom strand of site C (Fig. 2A, lanes 7 and 8), but there was a weak Mig1p footprint on the top strand (Fig. 2A, lanes 3 and 4); addition of 10 µg of recombinant Mig1p decreased the reactivity of C^{-205} and increased the reactivity of C^{-207}. Experiments using Mig1p partially purified from yeast extracts gave very similar results (Fig. 2B). Since the enhanced reactivity of C^{-128} on the bottom strand was the best indicator of Mig1p binding, we used it to monitor Mig1p binding *in vivo*. Figure 2B also shows that increasing amounts of Mig1p strengthened the footprint on the bottom strand of site A, showing that we could use the ratio of the intensity of C^{-128} to that of T^{-125} (which is not affected by Mig1p binding) as an approximate measure of Mig1p binding.

Mig1p binding to the *GAL4* promoter *in vitro*

Two Mig1p binding sites that contribute differently to glucose-induced repression of promoter activity (13) are also found in the *GAL4* promoter (3,13). Deletion or mutation of site 1 eliminates most repression while deletion or mutation of site 2 has only a small effect (13) and Mig1p binding to site 1 but not to site 2 has been detected by DNase I footprinting (3). We detected Mig1p

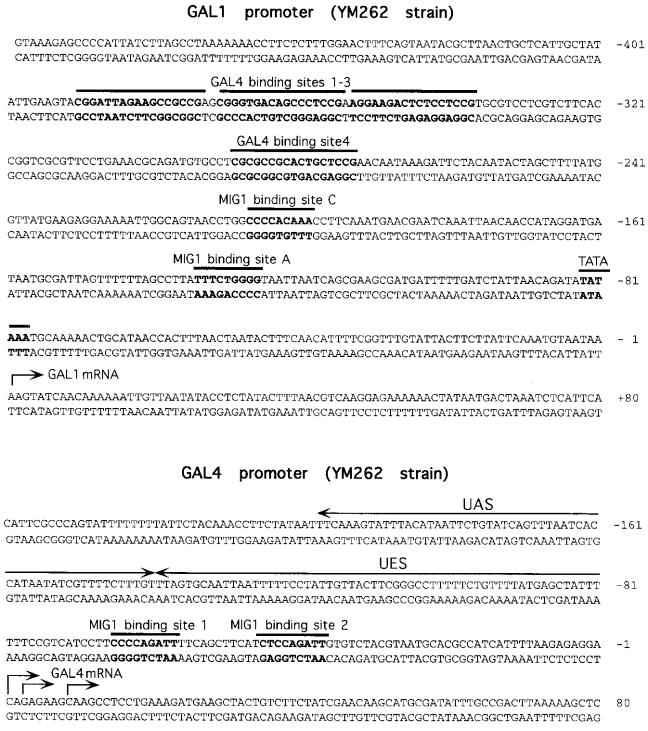

Figure 1. DNA sequences of the *GAL1* and *GAL4* promoters. Important sequence elements are indicated. They include: for the *GAL1* promoter, Gal4p binding sites 1–4 (21) and Mig1p binding sites A and C (3,32); for the *GAL4* promoter, UAS and UES activation sequences (14) and two Mig1p binding sites (3,14).

binding to both sites (bases –58 to –66 for site 1 and bases –38 to –46 for site 2) by DNase protection and by photofootprinting (Fig. 3). The UV pattern of the top strand of protein-free DNA (Fig. 3A, lane 6) showed two well-defined bands at site 1, C^{-66} and T^{-67}, and four weaker bands at site 2, C^{-43}, C^{-44}, T^{-45} and C^{-46}. Mig1p binding to site 1 resulted in a new band at C^{-65} and reduced the intensity of C^{-66} (Fig. 3A, lanes 7 and 8, and B). The Mig1p footprint at site 2 was more subtle and required more Mig1p; the intensities of C^{-43} and C^{-44} were reduced and that of T^{-45} was increased (Fig. 3A, lanes 7 and 8, and B). The bottom strand showed similar results (Fig. 3A, lanes 2–4). We conclude that Mig1p binds to both sites in the *GAL4* promoter, but with higher affinity to site 1. Since the Mig1p footprint on the top strand at site 1 was the clearest, we used cleavage at C^{-65} to monitor Mig1p binding to the *GAL4* promoter *in vivo*.

Footprinting *in vivo* of the *GAL1* promoter under induced and repressed conditions

Our previous analysis of the *GAL1* promoter by photofootprinting *in vivo* provided no evidence for Mig1p binding to the promoter under repressed or derepressed conditions. We repeated these experiments with strain YM262, in which expression of *GAL1* is rapidly repressed by the addition of glucose to cells growing on galactose. In agreement with our previous observations, addition of glucose to galactose-grown cells had little if any effect on the photofootprint (Fig. 4A, lanes 5 and 6).

To investigate this phenomenon further, we analyzed a second yeast strain, W303, in which expression of *GAL1* is only weakly

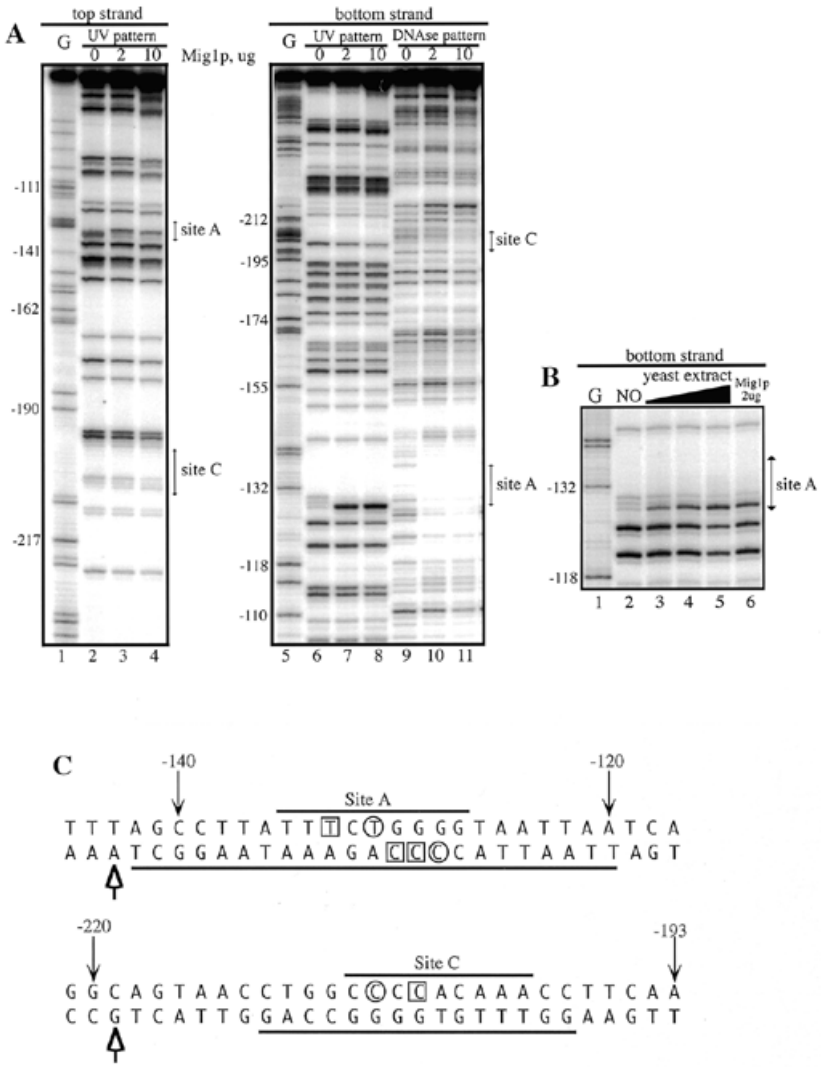

Figure 2. Mig1p binding *in vitro* to the *GAL1* promoter. (**A**) *In vitro* DNase I and UV footprints of Mig1p protein (truncated *E.coli* recombinant protein) bound to a *GAL1* promoter fragment (–312 to –27 relative to the transcription initiation site) labeled on either the top strand (lanes 1–4) or the bottom strand (lanes 5–11) as described in Materials and Methods. The samples were digested with DNase I (lanes 9–11) or irradiated with UV light for 2 min and subsequently cleaved at cyclobutane dimer sites with T4 endoV (lanes 2–4 and 6–8). The samples were then separated on a 6% acrylamide gel under denaturing conditions. Lanes 1 and 5 are Maxam–Gilbert G sequence markers. Mig1p binding sites are indicated. (**B**) UV footprints resulting from incubation *in vitro* of partially purified extracts from Mig1p overproducing yeast cells with the *GAL1* promoter fragment (labeled on the bottom strand). Lane 1, Maxam–Gilbert G reaction; lane 2, UV footprint of protein-free DNA; lanes 3–5, UV footprints with increasing amounts of Mig1p-enriched yeast extract; lane 6, UV footprint with 2 µg of truncated *E.coli* recombinant Mig1p. (**C**) Summary of UV footprinting and DNase I protection analyses of Mig1p/*GAL1* promoter interactions. Circled and boxed residues show sites of Mig1p-dependent enhanced and repressed endoV cleavage, respectively. Underlines indicate the DNase I-protected sequences and the arrows show DNase I-hypersensitive sites. Mig1p binding sites A and C are overlined.

repressed by glucose. In contrast to the result with YM262, we detected a clear photofootprint in W303 cells under repressing conditions (Fig. 4A, lane 4). The photofootprint must be due to Mig1p binding, since it did not appear in a W303 strain deleted for *MIG1* (data not shown). Northern blot analysis of *GAL1* mRNA revealed ~3-fold repression in W303 cells and >30-fold repression in YM262 cells, 30 min after adding glucose (data not shown). We concluded from these experiments that there was an unexpected inverse correlation between the Mig1p footprint at site A and the extent of glucose repression.

For YM262 and related strains, we have shown that addition of glucose to galactose-induced yeast cells induces a UV footprint between the UAS_{GAL} and the *GAL1* TATA element whose presence is associated with the formation of a positioned nucleosome between positions –258 and –92 (17,20,22,25). Because these sequences encompass the two Mig1p binding sites, we next asked whether the LMPCR UV footprint protocol would detect the same nucleosome-associated pattern after glucose repression of the *GAL1* promoter in the two strains used in this study. In the earlier experiments, we found that the clearest 'nucleosome footprint' was seen on the top strand between T^{-143} and T^{-146} (17). This footprint was not prominent in DNA from glucose-treated W303 cells (Fig. 4B, lane 4), which showed a pattern similar to that of protein-free DNA or DNA from

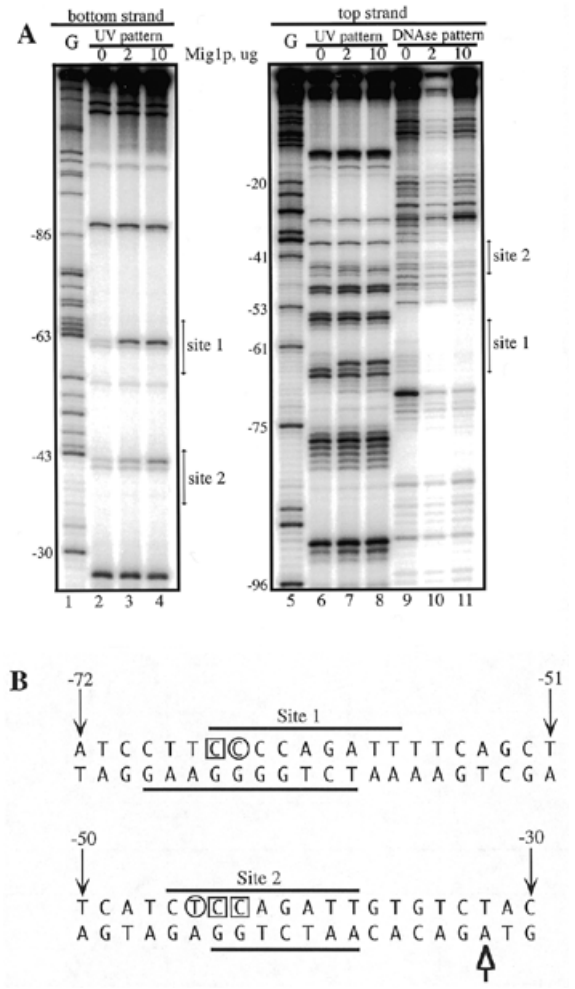

Figure 3. Mig1p binding *in vitro* to the *GAL4* promoter. (**A**) *In vitro* DNase I protection assays and UV footprints of Mig1p (truncated *E.coli* recombinant protein) bound to a *GAL4* promoter fragment labeled at the 3′-end of either the top strand (lines 1–4) or the bottom strand (lines 5–11) as described in Materials and Methods. Lane designations are identical to those in Figure 2A. (**B**) Summary of UV footprinting and DNase I protection analyses of the *GAL4* promoter. Indicated are sites of Mig1p-dependent enhanced (circled) and repressed (boxed) endoV cleavage. DNase-protected sequences are underlined and a DNase I-hypersensitive site is shown with an arrow. Mig1p binding sites 1 and 2 are overlined.

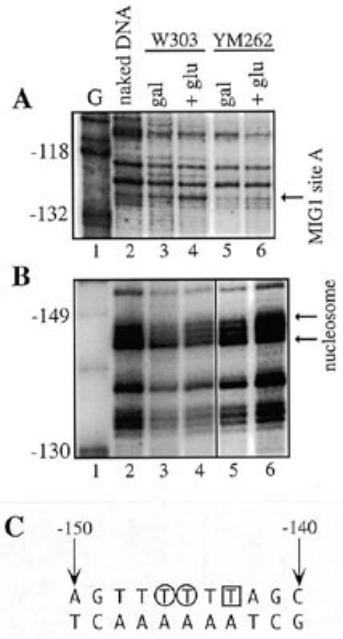

Figure 4. UV footprints of the *GAL1* promoter *in vivo*. Cells of W303 and YM262 strains were grown on YP galactose until OD_{600} = 2 and 50 ml portions were pelleted; the cells were resuspended in 3 ml of PBS buffer and irradiated for 1 min. To a second 50 ml aliquot glucose was added to 2% and the cells were allowed to grow for 30 min before they were pelleted and treated as described above. Control DNA was purified from untreated cells and UV irradiated in medium salt buffer. All DNAs were analyzed by LMPCR as described in Materials and Methods. (**A**) Bottom strand. Lane 1, G ladder; lane 2, UV irradiated protein-free DNA; lanes 3 and 4, UV irradiated W303 cells grown under induced or repressed conditions; lanes 5 and 6, UV irradiated YM262 cells. (**B**) Top strand. Lane assignment as in (A). (**C**) Summary of the *GAL1* promoter nucleosome UV footprint. Circled and boxed residues show sites of enhanced and repressed endoV cleavage.

galactose-grown cells (Fig. 4B, lanes 2 and 3). The same was not true for DNAs from the YM262 strain. Although the pattern for induced cells was the same as that for protein-free DNA (Fig. 4B, lane 5), addition of glucose resulted in decreased intensity of T^{-143} and increased intensities of T^{-145} and T^{-146} (Fig. 4B, lane 6; see also Fig. 5B). This pattern accompanies and is diagnostic for the packaging of those sequences into a positioned nucleosome (17,25). We conclude from these results that Mig1p probably binds only to nucleosome-free DNA and suggest that for the YM262 strain, chromatin remodeling during glucose repression prevents Mig1p binding to the *GAL1* promoter under fully repressed conditions.

To determine if the *GAL1* sequences between –258 and –92 of W303 cells can be incorporated into a nucleosome under any conditions, we examined the UV pattern of DNA isolated from

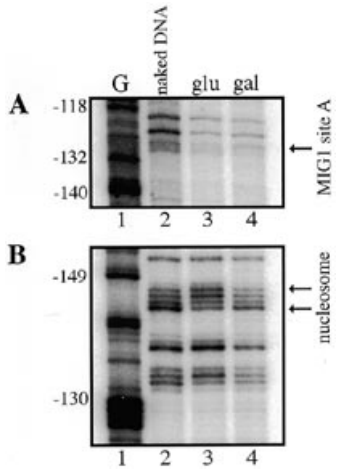

Figure 5. UV footprints of the W303 *GAL1* promoter *in vivo* after long-term growth in glucose. W303 cells were grown on glucose (lane 3) or galactose (lane 4) until the mid-logarithmic stage. Aliquots of 50 ml were pelleted and treated as described in Figure 4. (**A**) Bottom strand. Lane assignments are shown in the figure. (**B**) Top strand. Lane assignments as in (A).

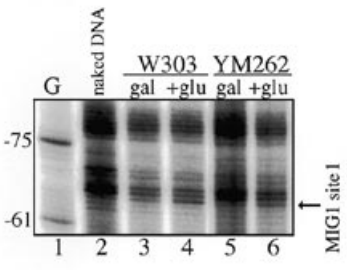

Figure 6. UV footprints of the top strand of the *GAL4* promoter *in vivo*. DNA used for LMPCR analysis was the same as in Figure 4. Primers are described in Materials and Methods.

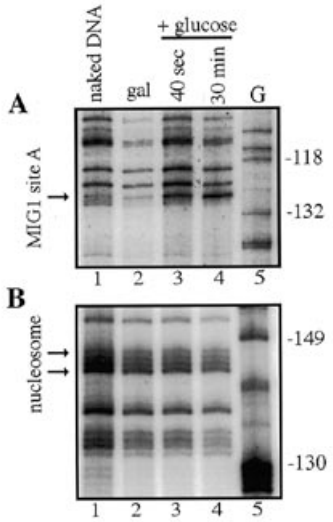

Figure 7. UV footprints of the *GAL1* promoter *in vivo* of a *gal80*$^{-}$ (YM654) strain during a transition from induced to repressed conditions. Cells were grown on SM galactose until OD_{600} = 2 and a 25 ml portion was irradiated for 1 min. Glucose to 2% was added to the remaining cells and 25 ml portions were harvested at the indicated time points and irradiated for 1 min. DNA was purified and treated as described in Figure 4. (**A**) Bottom strand. Lane 5, G ladder; lane 1, UV irradiated protein-free DNA; lane 2, cells grown in 2% galactose; lanes 3 and 4, cells grown for 40 s and 30 min, respectively, after addition of glucose to 2%. (**B**) Top Strand. Lane assignments as in (A).

W303 cells grown for an extended period of time in glucose. Under these conditions the promoter is rendered completely inactive, presumably a consequence of inhibition of Gal4p function by Gal80p and of decreased Gal4p levels resulting from glucose repression of the *GAL4* promoter. Under these conditions the UV pattern of the *GAL1* promoter top strand showed that it was incorporated into the positioned nucleosome (Fig. 5B, lane 3). There was no Mig1p footprint on the bottom strand (Fig. 5A, lane 3), consistent with the view that Mig1p binding is prevented by the nucleosome. As was seen previously (Fig. 4A, lane 3), LMPCR analysis of DNA from cells growing in galactose showed a faint Mig1p footprint on the bottom strand (Fig. 5A, lane 4) and no evidence for chromatin structure (Fig. 5B, lane 4).

Footprinting *in vivo* of the *GAL4* promoter under induced and repressed conditions

To explore the basis of the difference between the two strains, in particular the question of why we saw no Mig1p binding to the *GAL1* promoter in the YM262 background, we performed several experiments. First we looked at Mig1p binding to a different promoter. For this we chose the *GAL4* promoter, which is repressed by glucose in a *MIG1*-dependent manner, but never fully inactivated. We analyzed by LMPCR the same DNA samples that were used in the experiment presented in Figure 4. Figure 6 shows *in vivo* UV photofootprints of the top strand of the *GAL4* promoter. The band at position C^{-65} characteristic for Mig1p binding (see above) was visible in the UV pattern of DNA from galactose-induced W303 cells (Fig. 6, lane 3), but was not seen in DNA from equivalent YM262 cells (Fig. 6, lane 5), similar to results for the *GAL1* promoter (Fig. 4A, lanes 3 and 5). UV footprints on DNA from glucose-repressed cells were the same for both strains and were similar to that generated by Mig1p binding to site 1 *in vitro* (Fig. 6, lanes 4 and 6). (Binding to site 2 was not detected.) We conclude for both strains that Mig1p binding to the *GAL4* promoter is increased after addition of glucose to galactose-grown cells and that the extent of binding (at least to the *GAL4* promoter) is qualitatively similar.

Footprinting *in vivo* of the *GAL1* promoter under partially repressed conditions

We next tested the hypothesis that our failure to detect Mig1p binding to the YM262 *GAL1* promoter was because of its rapid transition to a repressed chromatin structure. To do this we determined if Mig1p binding to *GAL1* could be detected under conditions of partial repression, resulting either from elimination of Gal80p-dependent repression (15) or by using glucose concentrations that are not fully repressing. A weak Mig1p photofootprint, which was visible with DNA isolated from *gal80*$^{-}$ cells growing on 2% galactose (Fig. 7A, lane 3), was significantly intensified 40 s after adding glucose to 2% (Fig. 7A, lane 4) and persisted for 30 min (lane 5). Even after 30 min there was no indication of a nucleosome footprint at T^{-143} and T^{-146} (Fig. 7B). *GAL1* mRNA was reduced only 3-fold after 30 min in glucose (by northern blot analysis; data not shown). This reduction is 10-fold less than was seen in YM262 (*GAL80*$^{+}$) and similar to that seen in W303 cells.

In the experiments shown in Figure 4 we used high glucose concentrations (2%) to induce rapid repression of the YM262 *GAL1* promoter (in just 1 min; data not shown) and equally rapid formation of the positioned nucleosome. To effect partial repression, we repeated this experiment using lower glucose concentrations. YM262 cells were grown on 2% galactose until OD_{600} ~ 2, separated into aliquots and exposed to different glucose concentrations. After 30 min, samples from each aliquot were either irradiated with UV light and footprinted or used for analysis of *GAL1* and *GAL4* mRNA levels. Photofootprints from analysis of the *GAL1* promoter are shown in Figure 8A (top strand) and B (bottom strand). The Mig1p footprint was induced by 0.1 or 0.2% glucose, but higher glucose concentrations resulted in a weaker Mig1p footprint, with little or no footprint detectable in cells grown in 2 or 3% glucose. At the same time the UV pattern of the bottom strand showed the complementary appearance of the nucleosome footprint (Fig. 8B). UV footprinting of the *GAL4* promoter using the same DNA preparations showed a

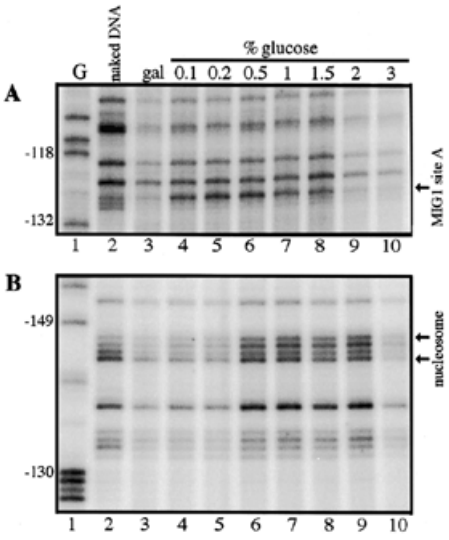

Figure 8. UV footprints of the *GAL1* promoter *in vivo* of YM262 cells grown in different glucose concentrations. Cells were grown on YP galactose until OD_{600} = 2, pelleted and resuspended in SM with 2% galactose. A 25ml aliquot was irradiated and appropriate amounts of glucose were added to 50 ml portions and cells were grown for another 30 min. An aliquot of 25 ml from each of these samples was irradiated and 25 ml was harvested for mRNA purification. After irradiation DNA from each sample was treated as described in Figure 4. (**A**) Bottom strand. Lane 1, G ladder; lane 2, UV irradiated protein-free DNA; lane 3, DNA from cells grown in 2% galactose; lanes 4–10, DNA from cells grown in 2% galactose plus 0.1, 0.2, 0.5, 1, 1.5, 2 and 3% glucose, respectively. (**B**) Top strand. Lane assignments as in (A).

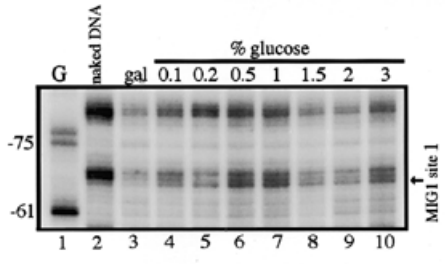

Figure 9. UV footprints of the *GAL4* promoter *in vivo* of YM262 cells grown in different glucose concentrations. DNA samples used in this experiment were the same as in Figure 8. Lane assignments are as in Figure 8.

parallel pattern of Mig1p binding at low glucose concentration (Fig. 9), but the footprint was retained at high glucose concentrations.

Figure 10A and B shows quantitation of the glucose dependence for *GAL1* mRNA, *GAL4* mRNA and Mig1p binding and nucleosome positioning at the *GAL1* promoter. [The intensities of the Mig1p footprints (band C^{-128}) were normalized to those of T^{-125}, which is unaffected by Mig1p binding (see above). The nucleosome footprint intensity is expressed as the ratio of band T^{-145} to band T^{-143}.] Mig1p binding increased rapidly with glucose concentration and reached a maximum between 0.2 and 0.5% glucose. The Mig1p footprint then decreased slowly and

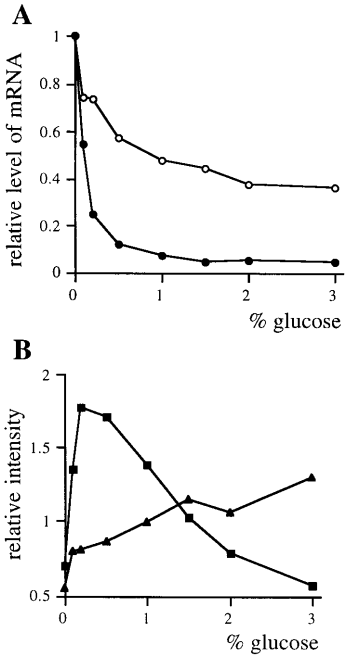

Figure 10. Effects of glucose concentration on mRNA levels and promoter structure. (**A**) Quantitation of *GAL1* (●) and *GAL4* (○) mRNA for the experiment described in Figure 8. The amount of mRNA was determined by northern blot analysis. Northern blots were quantified by phosphorimager analysis and normalized to the amount of *DED1* mRNA (17). The amount of mRNA is given as a fraction of the initial value at 0% glucose. (**B**) Quantitation of Mig1p binding (■) and nucleosome formation (▲) for the experiment described in Figure 8. The intensity of the Mig1p signal (band C^{-128}) was normalized to the intensity of the T^{-125} band, which is not affected by Mig1p binding. Nucleosome formation was determined as the ratio of band T^{-145} to band T^{-143}.

disappeared at high glucose. The nucleosome signal began to appear at 0.1% glucose and increased with increasing glucose concentration. Thus, Mig1p and the nucleosome apparently compete for the Mig1p binding site (URSA), with the nucleosome displacing Mig1p at high glucose concentrations. *GAL1* mRNA levels decreased rapidly and were maximally repressed (~20-fold) at 1.5% glucose. *GAL4* mRNA decreased more slowly and was 2.5-fold repressed at 2% glucose. We caution that the mRNA quantitation and DNA photofootprinting were carried out at a single time point (30 min after adding glucose) and repression by 0.1 or 0.2% glucose may be higher at later time points.

DISCUSSION

Cyclobutane dimer UV photofootprinting was an effective way to observe Mig1p binding to sequences in the *GAL1* and *GAL4* promoters. Although photofootprinting has not been widely used to investigate protein–DNA interactions, its application to analysis of eukaryotic gene regulation is relatively straightforward and it allows one to 'photograph' promoter structures during transitions between regulated states (17–19,27,33). By applying photofootprinting here, we followed the *GAL1* promoter as it was repressed by addition of glucose and found that binding of the glucose repressor Mig1p to the glucose-repressible *GAL1* and *GAL4* promoters was glucose-inducible *in vivo*. Although the details of the interaction were strain and promoter dependent, we conclude

that Mig1p association with the promoter plays an important early role in this switch, but does not appear to be part of a stably maintained repression complex.

Our first attempt at following the structure of the *GAL1* promoter during glucose repression confirmed previous results (17,22,25) showing that the switch is rapid and involves a transition from an open chromatin state to one in which a specific chromatin structure is formed, with no evidence of Mig1p binding under either condition. The strain we used was an S288c derivative which is subject to stringent glucose repression (1). Analysis of a different strain whose *GAL1* promoter is only weakly glucose repressed showed strong Mig1p binding under repressing conditions. Because parallel analysis of the *GAL4* promoter suggested that glucose-repressing conditions result in increased Mig1p binding, we reasoned that our inability to detect a Mig1p footprint at the *GAL1* promoter of the S288c strain reflected the rapid formation of a chromatin structure that prevented Mig1p binding. To test this hypothesis we performed the analysis under conditions where the promoter should be only partially repressed, in an S288c strain lacking *GAL80* and at lower glucose concentrations. Under each of these conditions we observed a glucose-dependent Mig1p footprint in the *GAL1* promoter, allowing us to conclude that Mig1p binding to glucose-repressed promoters is, in fact, regulated by glucose. A similar conclusion was drawn from analysis of binding of Mig1p to the *MAL62* promoter *in vivo* (34). Recent results show that a major source of this regulation comes from glucose-regulated Mig1p nuclear import and/or export (10). It is worth noting that glucose-regulated trafficking of Mig1p is independent of its association with Ssn6p and Tup1p (10). Consistent with this we saw our strongest Mig1p footprint in *ssn6*Δ cells, the only conditions where the footprint approached that of saturated binding *in vitro* (unpublished observations). Stronger binding under these conditions could result from a direct effect of Ssn6p/Tup1p on Mig1p binding, but we favor an indirect effect of Ssn6p/Tup1p repression on the competition between chromatin structure and Mig1p binding.

How does Mig1p binding regulate the *GAL1* and *GAL4* promoters? Repression by Mig1p requires both Ssn6p and Tup1p and Tup1p probably serves as the active repressor (5,6). Tup1p appears to interact with both chromatin components and with general transcription factors. Specifically, Tup1p anchored to DNA by α2 repressor promotes the formation of an ordered chromatin structure in flanking sequences (35–37) and Tup1p apparently binds directly to underacetylated H3 and H4 histone molecules (38). These interactions are sensitive to mutations in the N-termini of the two molecules that also interfere with normal Tup1p-mediated α2-dependent repression. For the *GAL1* promoter the chromatin structure associated with the fully repressed state is only seen under conditions where Mig1p is not bound, a result which superficially suggests a difference between repression by Mig1p and by α2 repressor. The mechanism of Mig1p-dependent repression of the *GAL4* promoter also appears to differ from that used by α2 since there are no apparent repression-associated chromatin structure changes (W.Horz and M.Johnston, unpublished results). Whether these repression mechanisms are really different is unclear. Repression by α2 is also affected by mutations in Srb10p(Are1p), a cyclin-dependent kinase-like molecule and a component of a mediator complex that associates with the C-terminal domain of the large subunit of PolII (39). Although the role of Srb10p and the mediator complex in repression is not known, we saw in our experiments that under conditions of partial repression, the increased Mig1p footprint was accompanied by a weakened TATA footprint (unpublished observations), presumably reflecting decreased TBP/TFIID binding. The relative contributions of changes in chromatin structure and changes in activator/general factor interactions to that altered footprint cannot be assessed.

Finally, complete repression of the *GAL1* promoter obviously requires not only the Mig1p repressor complex, but also the inactivation of Gal4p by Gal80p. Only when Gal80p is fully repressing does the chromatin structure form and prevent Mig1p access to its binding sites, and presumably general transcription factor access to the core promoter. Along this line, two points are worth noting. (i) Relatively low glucose concentrations (as low as 0.1%) were sufficient to induce Mig1p binding at the *GAL1* promoter of *GAL80* cells in the S288c background. Because the footprint at low glucose concentrations was similar to that seen with *gal80*$^{-}$ cells or with W303 cells at high glucose concentrations and because it appeared in parallel with the Mig1p footprint at the GAL4 promoter, we believe that relatively low glucose concentrations are sufficient to activate the Mig1p-dependent glucose repression pathway. Those same low concentrations are apparently insufficient to cause inhibition by Gal80p, which may respond to glucose through a pathway different from that of Mig1p. Recent studies suggest that Gal80p is regulated by interactions with a Gal3p/galactose/ATP complex (40–42). Potential mechanisms for glucose regulation of this complex include inducer exclusion, where glucose directly or indirectly inhibits transport of the inducer, galactose, into the cell or a direct effect of glucose or a glucose metabolite on the Gal3p/Gal80p complex. (ii) Although our goal was to monitor Mig1p binding in response to glucose, we also noted increased binding under other conditions, notably when cells were growing in minimal galactose medium compared with rich galactose medium (unpublished observations), suggesting that the signal delivered to promoters by Mig1p may be more complex than simply the external glucose concentration. A likely candidate for this signal is the intracellular AMP/ATP ratio or energy charge. Activity of the the mammalian AMP-activated protein kinase, a possible ortholog of the yeast SNF1 kinase, is responsive to the energy charge (43). Though AMP is probably not a direct SNF1 kinase effector, the energy charge may be the major determinant of SNF1 kinase activity (44).

In any case it is clear that rapid glucose repression of *GAL1* requires contributions from several repression systems. Although the ability of the *GAL1* promoter to transit between a fully repressed and a highly active state makes it a good system for studying these states, a full description of the mechanisms by which these transitions are made will have to include analysis of interactions between all of the actors in the transcription arena, DNA, general chromatin components, sequence-specific activators and repressors and general transcription factors.

ACKNOWLEDGEMENTS

We thank Mike Devit for a gift of recombinant Mig1 protein, Steve Lloyd for endonuclease V and Aziz Sancar for photolyase. This work was supported by a grant from the Washington University–Monsanto Agreement.

REFERENCES

1 Johnston,M. and Carlson,M. (1992) In Jones,E.W., Pringle,J.R. and Broach,J.R. (eds), *The Molecular and Cellular Biology of the Yeast Saccharomyces: Gene Expression*. Cold Spring Harbor Laboratory Press, Cold Spring Harbor, NY, Vol. 2, pp. 193–281.
2 Nehlin,J.O. and Ronne,H. (1990) *EMBO J.*, **9**, 2891–2898.
3 Nehlin,J.O., Carlberg,M. and Ronne,H. (1991) *EMBO J.*, **10**, 3373–3377.
4 Lundin,M., Nehlin,J.O. and Ronne,H. (1994) *Mol. Cell. Biol.*, **14**, 1979–1985.
5 Treitel,M.A. and Carlson,M. (1995) *Proc. Natl Acad. Sci. USA*, **92**, 3132–3136.
6 Keleher,C.A., Redd,M.J., Schultz,J., Carlson,M. and Johnson,A.D. (1992) *Cell*, **68**, 709–719.
7 Tzamarias,D. and Struhl,K. (1994) *Nature*, **369**, 758–761.
8 Celenza,J.L. and Carlson,M. (1986) *Science*, **233**, 1175–1180.
9 Tu,J. and Carlson,M. (1995) *EMBO J.*, **14**, 5939–5946.
10 De Vit,M., Waddle,J. and Johnston,M. (1997) *Mol. Biol. Cell*, **8**, 1603–1618.
11 Treitel,M.A., Kuchin,S. and Carlson,M. (1998) *Mol. Cell. Biol.*, **18**, 6273–6280.
12 Johnston,S.A., Zavortink,M.J., Debouck,C. and Hopper,J.E. (1986) *Proc. Natl Acad. Sci. USA*, **83**, 6553–6557.
13 Griggs,D.W. and Johnston,M. (1991) *Proc. Natl Acad. Sci. USA*, **88**, 8597–8601.
14 Griggs,D. and Johnston,M. (1993) *Mol. Cell. Biol.*, **13**, 4999–5009.
15 Johnston,M., Flick,J.S. and Pexton,T. (1994) *Mol. Cell. Biol.*, **14**, 3834–3841.
16 Lamphier,M.S. and Ptashne,M. (1992) *Proc. Natl Acad. Sci. USA*, **89**, 5922–5926.
17 Axelrod,J.D., Reagan,M.S. and Majors,J. (1993) *Genes Dev.*, **7**, 857–869.
18 Selleck,S.B. and Majors,J. (1987) *Nature*, **325**, 173–177.
19 Selleck,S.B. and Majors,J.E. (1987) *Mol. Cell. Biol.*, **7**, 3260–3267.
20 Selleck,S.B. and Majors,J. (1988) *Proc. Natl Acad. Sci. USA*, **85**, 5399–5403.
21 Giniger,E., Varnum,S.M. and Ptashne,M. (1985) *Cell*, **40**, 767–774.
22 Cavalli,G. and Thoma,F. (1993) *EMBO J.*, **12**, 4603–4613.
23 Lohr,D. and Hopper,J.E. (1985) *Nucleic Acids Res.*, **13**, 8409–8423.
24 Lohr,D. (1984) *Nucleic Acids Res.*, **12**, 8457–8474.
25 Reagan,M.S. and Majors,J.E. (1998) *Mol. Gen. Genet.* **259**, 142–149.
26 Axelrod,J.D. and Majors,J. (1989) *Nucleic Acids Res.*, **17**, 171–183.
27 Pfeifer,G., Drouin,R., Riggs,A. and Holmquist,G. (1992) *Mol. Cell. Biol.*, **12**, 1798–1804.
28 Mueller,P. and Wold,B. (1989) *Science*, **246**, 780–786.
29 Pfeifer,G., Drouin,R., Riggs,A. and Holmquist,G. (1991) *Proc. Natl Acad. Sci. USA*, **88**, 1374–1378.
30 Becker,M.M. and Wang,J.C. (1984) *Nature*, **309**, 682–687.
31 Becker,M.M. and Grossmann,G. (1992) *Methods Enzymol.*, **212**, 262–272.
32 Flick,J.S. and Johnston,M. (1990) *Mol. Cell. Biol.*, **10**, 4757–4769.
33 Axelrod,J.D., Majors,J. and Brandriss,M.C. (1991) *Mol. Cell. Biol.*, **11**, 564–567.
34 Wang,J., Sirenko,O. and Needleman,R. (1997) *J. Biol. Chem.*, **272**, 4613–4622.
35 Roth,S.Y., Shimizu,M., Johnson,L., Grunstein,M. and Simpson,R.T. (1992) *Genes Dev.*, **6**, 411–425.
36 Shimizu,M., Roth,S.Y., Szent,G.C. and Simpson,R.T. (1991) *EMBO J.*, **10**, 3033–3041.
37 Roth,S.Y., Dean,A. and Simpson,R.T. (1990) *Mol. Cell. Biol.*, **10**, 2247–2260.
38 Edmondson,D.G., Smith,M.M. and Roth,S.Y. (1996) *Genes Dev.*, **10**, 1247–1259.
39 Wahi,M. and Johnson,A.D. (1995) *Genetics*, **140**, 79–90.
40 Zenke,F.T., Engels,R., Vollenbroich,V., Meyer,J., Hollenberg,C.P. and Breunig,K.D. (1996) *Science*, **272**, 1662–1665.
41 Platt,A. and Reece,R.J. (1998) *EMBO J.*, **17**, 4086–4091.
42 Yano,K. and Fukasawa,T. (1997) *Proc. Natl Acad. Sci. USA*, **94**, 1721–1726.
43 Hardie,D.G. and Carling,D. (1997) *Eur. J. Biochem.*, **246**, 259–273.
44 Wilson,W.A., Hawley,S.A. and Hardie,D.G. (1996) *Curr. Biol.*, **6**, 1426–1434.